PHYSICAL REVIEW B VOLUME 16, NUMBER 9 1 NOVEMBER 1977

Anisotropy and magnetostriction of cobalt-substituted yttrium iron garnet

P. Hansen and W. Tolksdorf
Philips GmbH Forschungslaboratorium Hamburg, 2000 Hamburg 54, West Germany

R. Krishnan
Laboratoire de Magnetisme, Centre National de la Recherche Scientifique, 92 190 Bellevue, France

(Received 23 May 1977)

The anisotropy, magnetostriction, and ferromagnetic resonance linewidth of cobalt-substituted yttrium iron garnets of composition $Y_3Fe_{5-x-y}Co_xGe_yO_{12}$ have been investigated by means of ferromagnetic resonance at 9.15 GHz in the temperature range $4.2 \leq T \leq 500$ K. The impurities, the valence states, and the site distribution of the cobalt ions in the measured crystals have been determined by chemical analysis, optical absorption, and spin-echo measurements. The measured temperature dependence of both the anisotropy constants and the magnetostriction constants are compared with calculations performed in the framework of the single-ion theory. The behavior of the ferromagnetic resonance linewidth can be well interpreted on the basis of the calculated orientation dependence of the energy-level diagram within the longitudinal relaxation mechanism.

I. INTRODUCTION

The anisotropic behavior of cobalt ions has been investigated experimentally and theoretically in both garnets and ferrites for many years. However, for garnets there are no consistent experimental data of anisotropy and magnetostriction constants specifically with respect to the linear relationship between these constants and the total cobalt content. This situation is presumably caused by the problem that the cobalt ions may be present in different valence states and in addition are distributed over the different crystallographic sites where the actual distribution and valence states occuring in a single crystal are determined by the special growth conditions and the impurities present.

The separation of the magnetic contributions from these various configurations requires different analytical methods, detailed theoretical work, and the knowledge of the atomic parameters involved. These problems have been analyzed by Sturge *et al.*,[1,2] concerning essentially the magnetic anisotropy. The aim of this contribution is an extension of those discussions by presenting a set of consistent experimental data and some further theoretical aspects to improve the understanding of the anisotropic phenomena in particular of the Co^{2+} ions in garnets. In order to keep the Co^{3+} concentration quite low, germanium-compensated crystals have been used. Their anisotropic properties, like the magnetocrystalline anisotropy, the magnetostriction, and the resonance linewidth, show a pure linear dependence with increasing cobalt content over the complete temperature range $4.2 \leq T \leq 500$ K. This indicates the dominance of the Co^{2+} ions on octahedral sites and the negligible effect of Fe^{2+} ions in these crystals. This is confirmed by chemical analysis, optical absorption, and nuclear spin-echo measurements. The experimental results can be interpreted in terms of the single-ion model: however, no quantitative agreement was achieved. The resonance linewidth was characterized by typical temperature peaks and could be well understood by means of the longitudinal relaxation model as well as the calculated orientation dependence of the energy levels.

II. THEORY

The anisotropy and magnetostriction can be described phenomenologically by the dependence of the free energy on the direction of magnetization $\vec{\alpha}$ and the strain $\vec{\epsilon}$ by

$$F(\vec{\alpha}, \vec{\epsilon}) = F_0 + F_K(\vec{\alpha}) + F_{me}(\vec{\alpha}, \vec{\epsilon}) \ . \tag{1}$$

F_0 is a constant with respect to $\vec{\alpha}$, while $F_K(\vec{\alpha})$ represents the magnetocrystalline anisotropy and $F_{me}(\vec{\alpha}, \vec{\epsilon})$ is the magnetoelastic energy. It is convenient to express $F_K(\vec{\alpha})$ in terms of the direction cosines as

$$F_K(\vec{\alpha}) = K_1 s + K_2 p + K_3 s^2 + K_4 sp + \cdots \ , \tag{2}$$

where

$$s = \alpha_1^2\alpha_2^2 + \alpha_2^2\alpha_3^2 + \alpha_1^2\alpha_3^2 \ , \quad p = \alpha_1^2\alpha_2^2\alpha_3^2 \ .$$

The anisotropy constants K_i depend on temperature and composition. For garnets substituted by small amounts of transition-metal ions according to the formula $Y_3Fe_{5-x}M_xO_{12}$ the K_i can be decomposed as

$$K_i(T, x) = K_i(T, 0) + \Delta K_i(T, x) \ , \tag{3}$$

where $K_i(T, 0)$ represents the anisotropy constant

induced by the host and $\Delta K_i(T,x)$ arises from the substituted ion M. The magnetoelastic energy is given by

$$F_{me}(\vec{\alpha},\vec{\epsilon}) = -\tfrac{3}{2}\lambda_{100}(C_{11}-C_{12}) \times\left(\sum_{i=1}^{3}\alpha_i^2\beta_i^2 - \tfrac{1}{3}\right) - \tfrac{3}{2}\lambda_{111}C_{44} \times\sum_{k\neq i=1}^{3}\alpha_i\alpha_k\beta_i\beta_k \ . \quad (4)$$

The C_{ik} are the elastic constants and $\vec{\beta}$ denotes the direction of the strain. The magnetostriction constants λ_{hkl} can also be separated according to Eq. (3).

The single-ion theory[3,4] can be applied to calculate the anisotropy and the magnetostriction contribution ΔK_i and $\Delta\lambda_{hkl}$, respectively. Within the approximations employed in this model[2,5] the contribution to the free energy can be expressed as

$$\Delta F(\vec{\alpha},\vec{\epsilon}) = -\frac{kTN}{n}\sum_{i=1}^{n}\ln Z_i \ , \qquad Z_i = \sum_j \exp\left(-\frac{E_{ij}(\vec{\alpha},\vec{\epsilon})}{kT}\right) , \quad (5)$$

where N is the total number of Co^{2+} ions per cm^3 and a statistical distribution over the magnetically inequivalent octahedral sites ($n=4$) is assumed. $E_{ij}(\vec{\alpha},\vec{\epsilon})$ denotes the energy levels of these ions. The anisotropy contributions are related to the free energy ($\vec{\epsilon}=0$) by

$$\Delta K_1 = 4\{\Delta F([110]) - \Delta F([100])\} \ , \qquad \Delta K_2 = 9\{3\Delta F([111]) + \Delta F([100]) - 4\Delta F([110])\} \ , \quad (6)$$

provided the higher-order anisotropy constants are negligible. In the same manner the magnetostriction constants can be expressed by

$$\Delta\lambda_{100} = -\frac{2}{3}\frac{f_{33}([001]) - f_{33}([010])}{C_{11}-C_{12}} \ , \qquad \Delta\lambda_{111} = -\tfrac{1}{3}f_{12}([110])/C_{44} \ , \quad (7)$$

where

$$f_{ik}(\vec{\alpha}) = \frac{\partial\Delta F_{me}(\vec{\alpha},\vec{\epsilon})}{\partial\epsilon_{ik}} \ , \quad (8)$$

and again the two-constant energy expression is employed according to Eq. (4). The main effort in calculating the anisotropic behavior of the Co^{2+} ions thus concerns the determination of the dependence of the eigenvalues $E_{ij}(\vec{\alpha},\vec{\epsilon})$ on the direction of magnetization $\vec{\alpha}$ and the strain $\vec{\epsilon}$. Since the thermal energy in the temperature range $0 \leq T \leq T_C$ does not exceed energies of $kT_C \simeq 400\ cm^{-1}$, the temperature dependence of the anisotropy and magnetostriction contributions will be governed by the energy levels within this energy range. Thus, it is sufficient to analyze the level structure of the $^4T_{1g}$ cubic ground state. The 12-fold degeneracy of this state is removed by the following interactions:

$$\mathcal{H} = V_t(\vec{r}) + g\mu_B\vec{H}_{exch}\cdot\vec{S} + \lambda\vec{L}\cdot\vec{S} + \delta V(\vec{r},\vec{\epsilon}) \ . \quad (9)$$

$V_t(\vec{r})$ is the noncubic crystalline field arising from the local deformation of the octahedral sites in garnets. The second term represents the isotropic exchange interaction expressed in the molecular-field approximation. $\vec{S}$ is the spin operator of the Co^{2+} ion and the total spin is $S=\frac{3}{2}$. The exchange field $\vec{H}_{exch}$ has to be regarded as a function of temperature. The third term describes the spin-orbit coupling where $\vec{L}$ is the orbital momentum operator of the Co^{2+} ion and λ is the spin-orbit coupling constant. The last term represents the increment of crystalline field depending on strain and is much smaller than the other interactions and, therefore, can be neglected as far as the magnetic anisotropy is concerned. Since the Hamiltonian of Eq. (9) operates within the orbitally threefold degenerate $^4T_{1g}$ state which is mathematically isomorphic to a P state, it is convenient to introduce an effective angular momentum operator $\vec{L}'$ where the effective orbital states $|m_{L'}\rangle$ satisfy the relation[6]

$$L_z|m_{L'}\rangle = m_{L'}|m_{L'}\rangle, \quad m_{L'}=0,\pm1 \ ,$$

and the z axis is chosen along the local axis of deformation being one of the four [111] directions. In this representation the trigonal field can be replaced by $-\Delta_t(L_z'^2 - \frac{2}{3})$ where Δ_t is the trigonal field splitting and the spin-orbit term is written $-\alpha\lambda\vec{L}'\cdot\vec{S}$, where α depends on the relative magnitude of the trigonal field.[6] In case of $\Delta_t \gg g\mu_B H_{exch}$, $\alpha\lambda$, the eigenvalues and thus the anisotropy[7,8] and magnetostriction[9,10] contributions have been calculated and compared with experimental results of spinell ferrites. For garnets, however, it has been proved that this condition is not fulfilled[2] and that the eigenvalues have to be deduced from the full 12×12 matrix of the $^4T_{1g}$ state. Since our experimental data differ from those reported in Ref. 2 we have calculated the energy levels, from which the anisotropic properties can be deduced for arbitrary values of the trigonal field Δ_t, the exchange field H_{exch} and the effective spin-orbit coupling $\alpha\lambda$ in order to obtain the background necessary for discussing our experimental results. For the strain-free case and the special values $\Delta_t/g\mu_B H_{exch} = 2.5$ and $\alpha\lambda/g\mu_B H_{exch} = -0.538$ the energy level diagram is shown in Fig. 1, displaying also the orientation dependence in a $(1\bar{1}0)$ plane. The energies $E_{ij}(\vec{\alpha})$ can be labeled by the magnetic spin and orbital quantum numbers m_S and $m_{L'}$, respectively, as indicated on the right-hand side. The characteristics of this level structure will not change significantly as long as the parameters do not differ by more than one

magnitude. This diagram corresponds to the case where the quantization axis is along the [111] direction (γ_1 site) in the $(1\bar{1}0)$ plane. The dashed and dotted lines for the two lowest levels represent the orientation dependence at those sites with the quantization axis along the other [111] directions. The strong overlap of $m_{L'}=0$ and $m_{L'}=\pm 1$ wave functions are obvious from this representation which illustrates the necessity to take the complete ${}^4T_{1g}$ level structure into consideration. Near crossings of the levels occur at $\gamma_i = 90°$, where γ_i is the angle between the quantization axis ([111] directions) and the direction of magnetization. For $\vec{M}$ in the $(1\bar{1}0)$ plane this applies to the [110] and the [112] directions giving rise to strong relaxation which will be discussed in Sec. III D.

The anisotropy contributions have been obtained using Eqs. (5), (6), and (9). The result is shown in Fig. 2 where the ratio $\Delta K_2/\Delta K_1$ is plotted versus $-\alpha\lambda/g\mu_B H_{\text{exch}}$ for different values of $\Delta_t/g\mu_B H_{\text{exch}}$ at $T=0$. The dashed line represents the case discussed in Ref. 2. For large trigonal fields ($\Delta_t \gg g\mu_B H_{\text{exch}}$, $\alpha\lambda$) the ratio $\Delta K_2/\Delta K_1$ is considerably larger than the experimental value indicated by the dotted line. To estimate the parameters Δ_t, $g\mu_B H_{\text{exch}}$, and $\alpha\lambda$ the absolute magnitude of the ΔK_i has to be known as well. For $\Delta K_2/\Delta K_1 = -4.5$ (dotted line in Fig. 1) the dependence of $\Delta K_2/N$ on $g\mu_B H_{\text{exch}}$ is displayed in Fig. 3 for various Δ_t values at $T=0$ K. The observed K_2/N value is indicated by the dashed line. From the comparison of these representations and the experimental results the ratios $\alpha\lambda/g\mu_B H_{\text{exch}}$ and $\Delta_t/g\mu_B H_{\text{exch}}$ can be determined while the absolute magnitude of these pa-

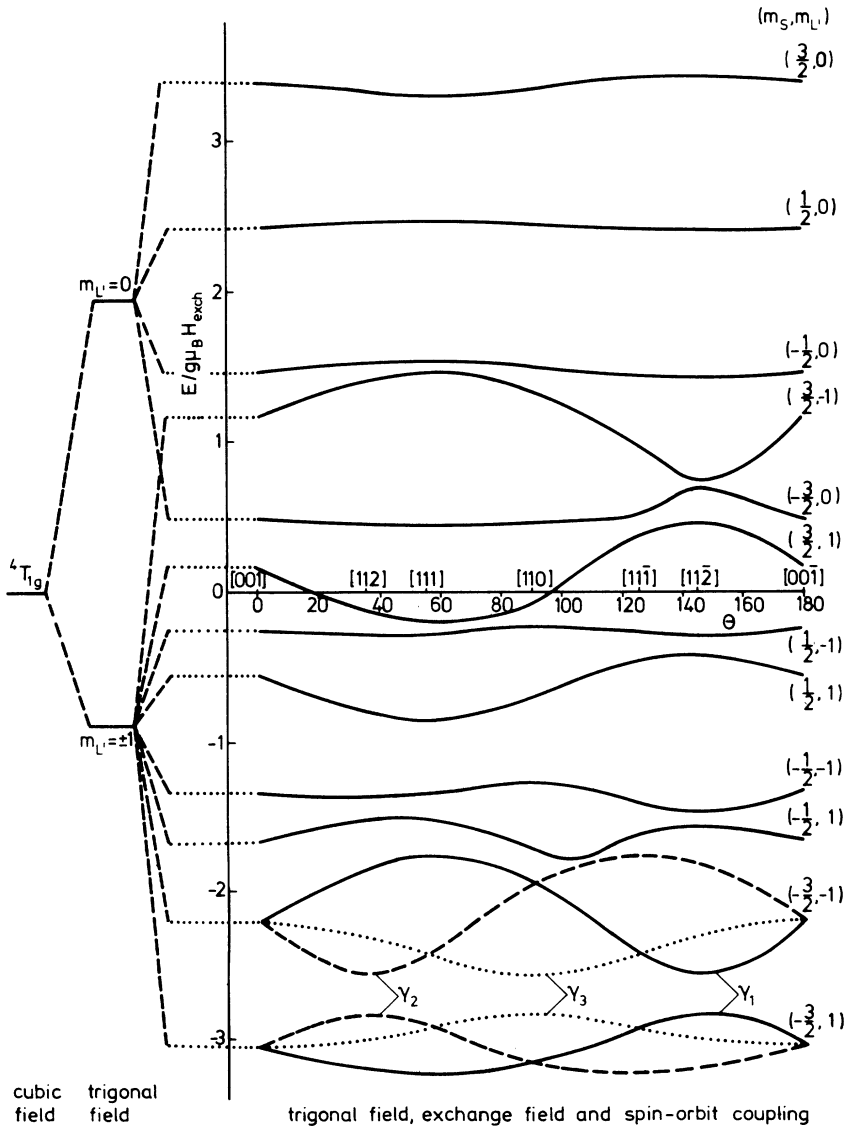

FIG. 1. Splitting of the ${}^4T_{1g}$ cubic ground state of a Co^{2+} ion on an octahedral site with the quantization axis along the [111] direction (γ_1 site). The energy levels are labeled by the magnetic spin and orbital quantum numbers m_S and m'_L, respectively. The orientation dependence of the energy levels refers to a variation of the direction of magnetization in the $(1\bar{1}0)$ plane. The dashed and dotted lines of the two lowest levels represent the variation at the magnetically inequivalent octahedral sites with a quantization axis along the $[1\bar{1}\bar{1}]$ axis (γ_2 site) and along the $[\bar{1}11]$ or $[1\bar{1}1]$ direction (γ_3 or γ_4 site), respectively.

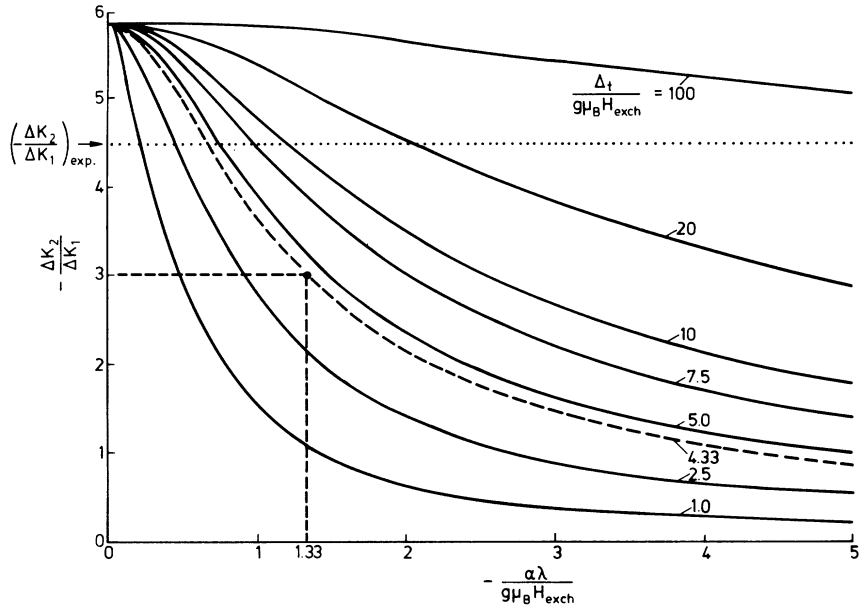

FIG. 2. Ratio of the anisotropy contributions ΔK_i of octahedral Co^{2+} ions vs the ratio of the spin-orbit coupling energy and the exchange energy for various values of the reduced trigonal field. The point indicated by the dashed lines was discussed in Ref. 2. The dotted line represents the average measured value of this work.

rameters can be estimated from the fit of the measured temperature dependence.

The magnetostriction can be calculated by perturbation theory[9-11] since the increment of crystalline field $\delta V(\vec{r},\vec{\epsilon})$ depending on strain is much smaller than the other interactions of the Hamiltonian of Eq. (9). This procedure, however, requires the knowledge of the unperturbed $|m_{L'}, m_S\rangle$ wave functions which are not explicitly known, except for the case $\Delta_t \gg g\mu_B H_{exch}, \alpha\lambda$. Therefore, we will derive an approximate relation for the temperature dependence of the magnetostriction contributions $\Delta\lambda_{hkl}$. For small $\delta V(\vec{r},\vec{\epsilon})$ the energy $E_{ij}(\vec{\alpha},\vec{\epsilon})$ can be decomposed by

$$E_{ij}(\vec{\alpha},\vec{\epsilon}) = E_{ij}(\vec{\alpha}) + \delta E_{ij}(\vec{\alpha},\vec{\epsilon}) = g\mu_B H_{exch}\,[e_{ij}(\vec{\alpha}) + \delta e_{ij}(\vec{\alpha},\vec{\epsilon})]\,, \tag{10}$$

where $\delta E_{ij}(\vec{\alpha},\vec{\epsilon}) \ll E_{ij}(\vec{\alpha})$ is proportional to the matrix element $\langle m_{L'}, m_{S'}|\,\delta V(\vec{r},\vec{\epsilon})|m_{L''}, m_{S''}\rangle$. With the aid of Eqs. (5), (8), and (10), and considering only the two lowest energy levels, we obtain

$$f_{ik}(\vec{\alpha}) = -\frac{N}{8}\sum_{i=1}^{4}\frac{\partial\,\delta\Delta E_i}{\partial\epsilon_{ij}}\tanh\left(\frac{\Delta E_i}{2kT}\right)\,. \tag{11}$$

The energy separation $\Delta E_i(\vec{\alpha},\vec{\epsilon}) = \Delta E_i(\vec{\alpha}) + \delta\Delta E_i(\vec{\alpha},\vec{\epsilon})$, in addition, has been approximated by

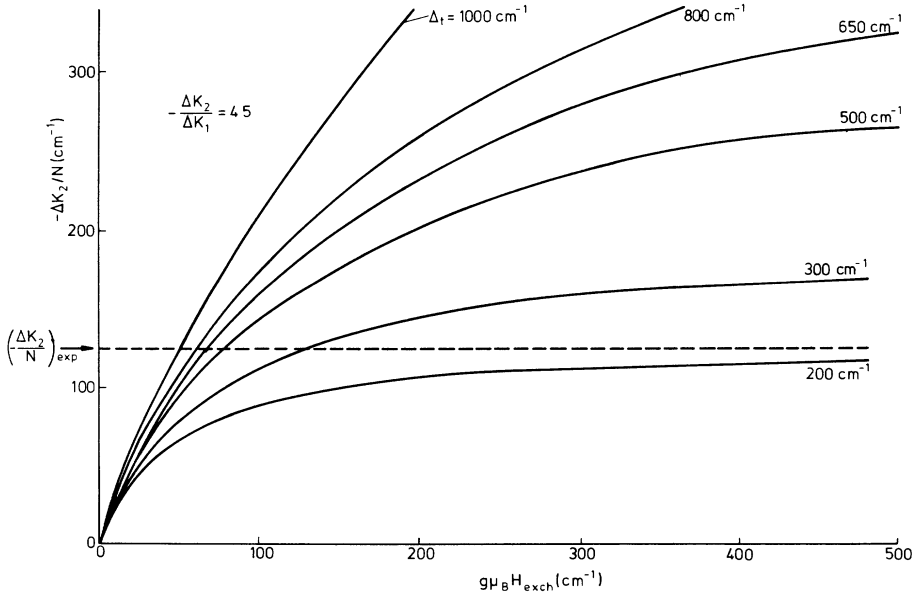

FIG. 3. Absolute value of K_2/N vs exchange energy for $\Delta K_2/\Delta K_1 = -4.5$ (this value refers to the dotted line in Fig. 2) and various trigonal field splittings.

a symmetric splitting which is the case if the angular variation of the $(-\frac{3}{2}, -1)$ level is replaced by that of the corresponding $(-\frac{3}{2}, 1)$ level. Since the ΔE_i are equivalent for $\vec{\alpha} \| [100]$ the magnetostriction contribution $\Delta\lambda_{100}$ can be expressed within this approximation by

$$\Delta\lambda_{100}(T) = \Delta\lambda_{100}(0) q(T) \tanh\left(\frac{\Delta E(\gamma_1)}{2kT}\right). \quad (12)$$

$\Delta E(\gamma_1)$ is the energy separation for $\vec{\alpha} \| [100]$ where $\gamma_i = 54.73°$. $q(T)$ represents the temperature dependence of the exchange field which for octahedral ions can be approximated by the relative temperature dependence of the tetrahedral sublattice magnetization. $\Delta\lambda_{100}(0)$ includes all constants and in particular is proportional to N and the derivative of the matrix element over $\delta V(\vec{r}, \vec{\epsilon})$ with respect to the strain components where the latter is not known from independent measurements. Thus $\Delta\lambda_{100}(0)$ has to be regarded as an adjustable parameter.

For $\Delta\lambda_{111}(T)$ the expression becomes more complicated, since two different sites have to be considered for $\vec{\alpha} \| [110]$. In this case we find

$$\Delta\lambda_{111}(T) = \frac{\Delta\lambda_{111}(0) q(T)}{1+C}\left[\tanh\left(\frac{\Delta E(\gamma_2)}{2kT}\right) + C \tanh\left(\frac{\Delta E(\gamma_3)}{2kT}\right)\right], \quad (13)$$

where $\Delta E(\gamma_2)$ and $\Delta E(\gamma_3)$ are the energy splitting of the two lowest levels for $\gamma_2 = 35.27°$ and $\gamma_3 = 90°$, respectively. C depends on the matrix elements of $\delta V(\vec{r}, \vec{\epsilon})$ and the other atomic parameters involved.

III. EXPERIMENTAL RESULTS AND DISCUSSION

A. Characterization of single crystals

Single crystals of composition $Y_3Fe_{5-x-y}Co_xGe_yO_{12}$ were grown by the flux method with a cooling rate of 0.5 °C/h from 1120 to 1000 °C, when they were separated from the flux by turning the platinum crucible upside down.[12,13] A typical melt composition in weight percent was PbO: 39.08; PbF_2: 31.94; B_2O_3: 1.81; Fe_2O_3: 2.7, and 24.47 oxides forming the yttrium iron-cobalt-germanium garnet. The yield was about 15 g consisting of regularly shaped crystals, up to 1 cm in size. The rare-earth impurity content in the starting materials was below 1 ppm. Inclusion free samples have been selected for all measurements. The analysis data and the values x_0 and y_0 of the starting composition are summarized in Table I. The total cobalt and germanium content was measured directly on polished platelets by x-ray fluorescence analysis using dense polycrystalline garnet materials for calibration. The cobalt content additionally has been determined by atomic absorption. Within the given error the results of both methods are in good agreement. The analysis of the impurities Si^{4+}, Pb^{2+}, Ca^{2+}, Fe^{2+}, F^- have been described previously.[13,14] The given error limits include the inhomogeneity of the distribution of the analyzed ions owing to the growth process.

From these data it is obvious that the excess of Ge^{4+} is not necessarily compensated by Fe^{2+} ions which are present in a low concentration. The presence of Fe^{2+} is important for the discussion of the magnetic behavior since these ions give rise to pronounced contributions to the magnetostrictive effects.[14-17] This low-Fe^{2+} contribution is also confirmed by optical absorption measurements shown in Fig. 4, and by ferromagnetic resonance linewidth and spin-wave linewidth measurements given in Table II. The optical absorption of Fe^{2+} containing yttrium iron garnet is considerably increased below 2.5 μm.[14] From a comparison of the data presented in Fig. 4 and those reported in Ref. 14, the Fe^{2+} contribution is estimated to be negligibly small. In addition, the height of the peak in the temperature dependence of the linewidth at

TABLE I. Analysis data per formula unit of the measured garnet single crystals of composition $Y_3Fe_{5-x-y}Co_xGe_yO_{12}$. x_0 and y_0 refer to the starting composition.

Sample No.	x_0	y_0	x	y	Impurities Si^{4+}	Pb^{2+}	Ca^{2+}	Fe^{2+}	F^-
1	0	0	0	0	0.002	0.015	0.001	0.006	0.014
2	0.025	0.025	0.003	0.018	0.002	0.015	0.0008	0.016	0.005
3	0.050	0.050	0.007	0.025	0.007	0.015	•••	0.015	0.006
4[a]	0.10	0.10	0.009	•••	0.013[b]	0.009[b]	0.0013[b]	•••	0.002[b]
5	0.10	0.10	0.018	0.042	0.002	0.022	0.0007	0.010	0.004
6	0.20	0.20	0.043	0.076	0.003	0.030	0.0008	0.010	0.004
error	•••	•••	±0.0005	±0.001	±0.001	±0.002	±0.0005	±0.004	±0.003

[a] Sample No. 4 has been grown by R. Krishnan under essentially the same growth conditions, except for the melt composition exhibiting a higher surplus of Fe_2O_3.

[b] Analyzed by W. Tolksdorf.

$T = 370$ K is a very sensitive measure of the presence of Fe^{2+} ions[14,18] which was not easily observable in these crystals (see Sec. III D, Fig. 13). These linewidth data indicate that the actual concentration of magnetically active Fe^{2+} ions on octahedral sites is very small. This behavior is found for most crystals and in particular for pure yttrium iron garnets and indicates that part of the Fe^{2+} ions presumably occupy dodecahedral sites where they contribute much less to the anisotropic properties.

Thus the main problem in the interpretation of the anisotropic properties will arise from the cobalt ions which may be present in different valence states. These have been studied by spin-echo measurements[19] which have been successfully applied to distinguish the valence states of cobalt ions in garnets.[20] The result is presented in Table II for two typical samples. Sample No. 5 exhibits a very low concentration of tetrahedral Co^{2+} and Co^{3+} ions. The other crystals, except for sample No. 4 grown by R. Krishnan, are expected to behave similarly since on the one hand they are grown under the very same conditions and on the other hand all measured properties are strictly linear with respect to the total cobalt content. This is particularly obvious from the spin-wave linewidth given in Table II and plotted in Fig. 12 which is a very sensitive measure for the presence of anisotropic ions. Therefore, we can assume that these crystals essentially are characterized by the same ratio of octahedral Co^{2+} ion and tetrahedral Co^{2+} and Co^{3+} ions. The concentrations of the two latter are very small and negligible in the discussion of anisotropy and magnetostriction since their contribution to anisotropic effects is quite small.[2] Sample No. 4 has a relatively high Co^{3+} content.

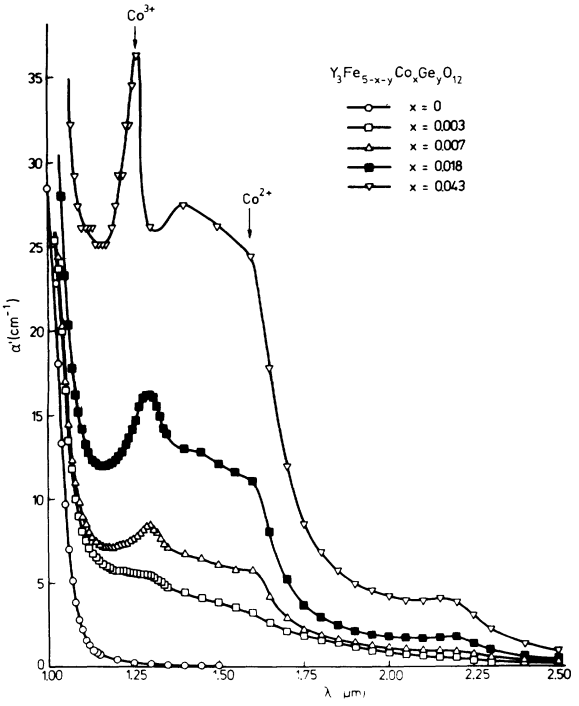

FIG. 4. Room-temperature optical absorption of cobalt-substituted yttrium-iron-garnet single crystals. α' is defined by $\alpha' = 0.43\ \alpha = (0.43/t)\ln(I_0/I)$, where t is the thickness of the platelet and I_0/I the relative intensity of the light corrected with respect to interface reflections. The peak at 1.3 μm and the shoulder at 1.6 μm are due to tetrahedral Co^{3+} and tetrahedral Co^{2+}, respectively.

TABLE II. Total cobalt content (Table I), tetrahedral Co^{3+}, and octahedral Co^{2+} content determined from spin-echo measurements (Refs. 19 and 20), ferromagnetic resonance linewidth and spin-wave linewidth ΔH_k in [111] direction at 9.15 GHz and $T = 295$ K. The ΔH data are not corrected for the cavity losses being roughly 0.2 Oe.

Sample	x	Co^{2+} [a]	Co^{3+} [b]	ΔH_k (Oe)	ΔH (Oe)
1	0	0	0	0.15	0.75
2	0.003	...	...	2.81	4.7
3	0.007	...	...	7.33	11
4	0.009	0.006	0.0018	5.92	11.5
5	0.018	0.17	0.0005	19.64	29
6	0.043	...	...	...	70

[a] Octahedral site.
[b] Tetrahedral site.

This distribution of cobalt ions of different valence states is reflected in the optical absorption at room temperature presented in Fig. 4. The optical-transmission measurements were performed with a Zeiss PMQ II spectrometer using platelets of about 0.1-cm thickness. The absorption peak at 1.3 μm originates from the low content of Co^{3+} ions on tetrahedral sites[2,21] owing to the high oscillator strength. The shoulder at 1.6 μm can be attributed to the tetrahedral Co^{2+} ions.[2] The spectrum became more characteristic at $T = 4.2$ K where the 1.6-μm peak appears more pronounced.

B. Anisotropy

The anisotropy has been measured by ferromagnetic resonance at about 9.15 GHz in the temperature range $4.2 \leq T \leq 500$ K. Spheres of 0.07-cm diameter have been used which were oriented with a [110] direction as an axis of rotation such that the applied dc field and thus the direction of magnetization is in the $(1\bar{1}0)$ plane. The field for ferromagnetic resonance is recorded continuously[5] and a typical plot of the orientation dependence in the

$(1\bar{1}0)$ plane is displayed in Fig. 5. The strong peaks in the [110] and [112] directions can be assigned to the near crossings of the energy levels at these directions for the magnetically different octahedral sites of the Co^{2+} ions (as shown in Fig. 1). The resonance condition for spherical samples can be expressed by[22,23]

$$\omega = \gamma_e [(H_r + H_K^x)(H_r + H_K^y)]^{1/2} ,$$
$$H_K^x = \frac{1}{M_s} \frac{\partial^2 F}{\partial \theta^2} , \tag{14}$$
$$H_K^y = \frac{1}{M_s} \left(\cot\theta \frac{\partial F}{\partial \theta} + \frac{1}{\sin^2\theta} \frac{\partial^2 F}{\partial \varphi^2} \right) ,$$

where γ_e denotes the effective gyromagnetic ratio. With the aid of Eqs. (1), and (5) the anisotropy fields and thus the resonance field at constant frequency can be calculated provided the orientation dependence of the energy levels is known. However, from Eq. (14) and the level structure it is obvious that the anisotropy fields are minimal at the [110] and [112] directions for the respective sites when the resonance field reaches its maximum value. This strong orientation dependence induced by these near crossings cause a strong anisotropy contribution. Restricting ourselves to the two constant theory, the K_1 and K_2 have been evaluated from the well-known relations

$$\omega = \gamma_e \{H_r([001]) - 2K_1/M_s\} ,$$
$$\omega = \gamma_e \{H_r([111]) - \tfrac{4}{3}K_1/M_s - \tfrac{4}{9}K_2/M_s\} ,$$
$$\omega = \gamma_e \{H_r([110]) - 2K_1/M_s\}^{1/2} \tag{15}$$
$$\times \{H_r([110]) + K_1/M_s + \tfrac{1}{2}K_2/M_s\}^{1/2} ,$$

which are easily derived from Eqs. (2) and (14).

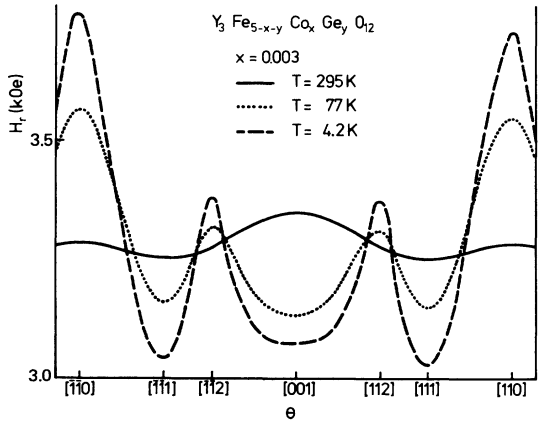

FIG. 5. Field for ferromagnetic resonance of cobalt-substituted yttrium iron garnet being continuously recorded in a $(1\bar{1}0)$ plane for different temperatures for sample No. 2.

The saturation magnetization M_s turns out to be unchanged by the small cobalt substitutions within experimental error. The measured temperature dependence of the anisotropy constants deduced from these relations is shown in Figs. 6(a) and 6(b). The magnitude and temperature dependence are essentially similar to those reported by Okada *et al.*[24] for the same garnet system whereas room temperature data reported for cobalt-silicon-doped

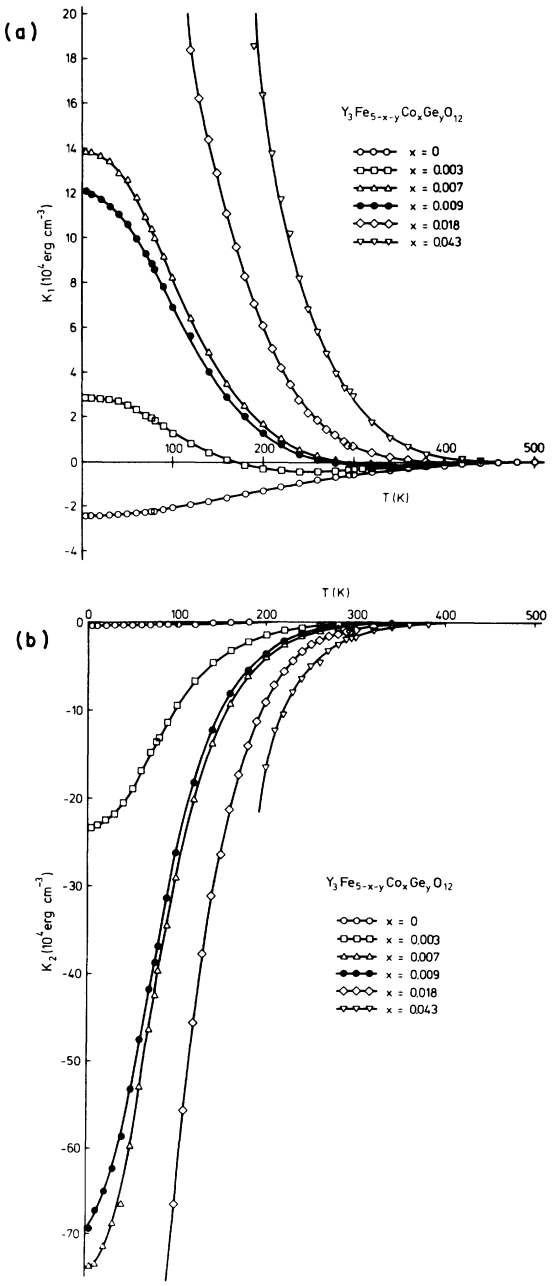

FIG. 6. Temperature variation of (a) K_1 and (b) K_2 for cobalt-substituted yttrium iron garnets.

yttrium iron garnet are smaller by a factor of 3 as compared to those of Ref. 25. For samples with a higher cobalt content the anisotropy and linewidth become too large for accurate measurements. The anisotropy of sample No. 4 which contains a larger amount of tetrahedral Co^{2+} and Co^{3+} is in accordance with the octahedral Co^{2+} content being $x = 0.0066$ as indicated in Table II. The same result is obtained from the comparison of the spin-wave linewidth data. From Table II or Fig. 12 the Co^{2+} content of this sample can be estimated to be $x = 0.006$, assuming the linewidth contribution of tetrahedral Co^{2+} and Co^{3+} is negligibly small owing to their level structure.[2] From this sample with higher Co^{3+} content the anisotropy and magnetostrictive effects of the Co^{3+} ions can be discussed and will be reported in a separate publication.[26] The concentration dependence of the anisotropy constants is shown in Fig. 7 for two temperatures. The linear relationship is well accomplished. From these data the per ion contributions can be calculated. The results are summarized in Table III where the data for the anisotropic ions Fe^{2+} (Ref. 14) and Ru^{3+} (Refs. 27–29) in particular are also presented for comparison. The much smaller Fe^{2+} contributions and the low-Fe^{2+} concentration justifies neglecting the Fe^{2+} effects with respect to magnetic anisotropy in these crystals. The Ru^{3+} ions give rise to comparable anisotropy contributions at low temperatures. At higher temperatures they lead to larger anisotropy constants owing to a weaker temperature dependence caused by the very different energy level structure of the Ru^{3+} ions.

The magnitude and the temperature dependence can be calculated as discussed in Sec. II. For a pure single-ion behavior the anisotropy contributions should show a linear concentration dependence or the ratio $\Delta K_2/\Delta K_1$ should be independent of concentration. This is fulfilled for all samples leading to the same temperature dependence of $\Delta K_2/\Delta K_1$, as shown in Fig. 8. These data can be compared with the theory outlined in Sec. II. The temperature dependence of the exchange field has been assumed to vary with the tetrahedral sublat-

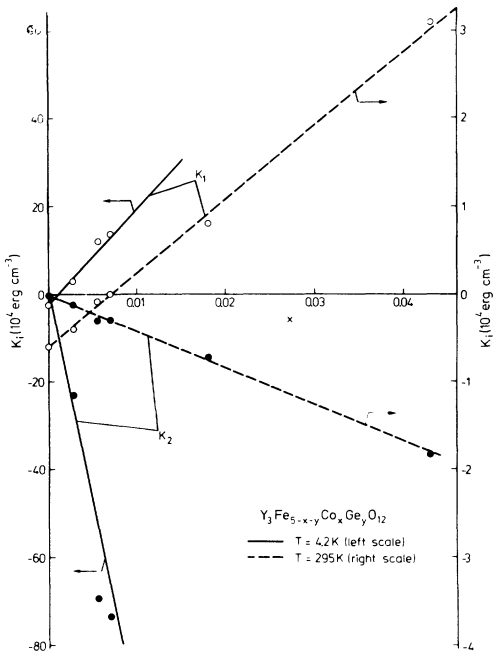

FIG. 7. Concentration dependence of the anistropy constants for cobalt-substituted yttrium iron garnets at $T = 4.2$ K and $T = 295$ K.

TABLE III. Anisotropy and magnetostriction contribution of magnetically anisotropic transition-metal ions substituted on octahedral sites in yttrium iron garnet.

Ion	Configuration	Cubic ground state	T (K)	Anisotropy $\Delta K_1/N$ (cm^{-1})	Anisotropy $\Delta K_2/N$ (cm^{-1})	Magnetostriction $10^4\Delta\lambda_{100}/x$	Magnetostriction $10^4\Delta\lambda_{111}/x$	Reference
Co^{2+}	$3d^7$	$^4T_{1g}$	4.2	27	−124	−0.5	1.0	This work
			77	21	−71	−0.6	1.2	
			295	1.0	−0.5	−0.4	0.7	
Ru^{3+}	$4d^5$	$^2T_{2g}$	4.2	28	−120	2.7[a]	2.9[a]	
			77	22	−68	2.7[a]	2.6[a]	11, 29
			295	2	−3	2.5[a]	0.8[a]	
Fe^{2+}	$3d^6$	$^5T_{2g}$	4.2	4.5	−13	1.7	7.1	
			77	2.3	−4.1	3.2	9.3	14, 17
			295	0.1	−0.1	0.5	1.4	
Mn^{3+}	$3d^4$	^5E_g	77	0.06	...	1.4	−0.24	41
			295	0.01	−0.006	0.7	+0.14	42

[a]Higher values have been reported for Ru-doped yttrium iron garnets measured by a static method (Ref. 43).

tice magnetization. The case $\Delta_t \gg g\mu_B H_{\text{exch}}$, $\alpha\lambda$ successfully applied by Slonczewski to cobalt-substituted spinell ferrites in the high-temperature range[7,30,31] is shown by the dotted line using the values $g\mu_B H_{ex} = 250\ \text{cm}^{-1}$ and $\alpha\lambda = -120\ \text{cm}^{-1}$. A very good fit can be achieved in the temperature range $50\ \text{K} \leq T \leq T_C$, however, at low temperatures, the ratio $\Delta K_2/\Delta K_1$ cannot be described satisfactorily and in addition the absolute magnitude is larger by a factor of 4. This is obvious also from Fig. 3. The temperature dependence discussed by Sturge *et al.*[2] was calculated with the parameter values $\Delta_t = 650\ \text{cm}^{-1}$, $g\mu_B H_{\text{exch}} = 150\ \text{cm}^{-1}$ and $\alpha\lambda = -200\ \text{cm}^{-1}$ leading to the dashed curve. These data are not in accordance with our experimental results. In particular we observed a larger ΔK_2 value giving rise to a larger $\Delta K_2/\Delta K_1$. From the average experimental value $\Delta K_2/\Delta K_1 = -4.5$ at $T = 4.2$ K the range of possible parameter values of $\Delta_t/g\mu_B H_{\text{exch}}$ and $\alpha\lambda/g\mu_B H_{\text{exch}}$ is indicated in Fig. 2. In addition, the absolute value of the ΔK_i being displayed in Fig. 3 has to be considered for selection of the parameters which describe the experimental results. It turns out that for $\Delta K_2/\Delta K_1 < -4$ there is no set of parameters which fits the measured ΔK_i and their ratio better than 20%, which becomes even worse for increasing $|\Delta K_2/\Delta K_1|$. While the complete temperature dependence of $\Delta K_2/\Delta K_1$ could be fitted excellently, the absolute values at $T = 4.2$ K disagree roughly by a factor of 3. The continuous line in Fig. 8 has been calculated for $\Delta_t = 650\ \text{cm}^{-1}$, $g\mu_B H_{\text{exch}} = 260\ \text{cm}^{-1}$, and $\alpha\lambda = -140\ \text{cm}^{-1}$, where the trigonal field splitting have been determined by Sturge *et al.*[1] For these parameters the $\Delta K_2/\Delta K_1$ data and those for ΔK_i above 100 K are described within 30% accuracy but for $T = 0$ K there is still a disagreement by approximately a factor of 2 between theory and experiment in the absolute ΔK_i values. This discrepancy may be attributed to the Coulomb interaction between the Co^{2+} ions and the charge compensating Ge^{4+} ions where the latter is expected to be of the order $50-100\ \text{cm}^{-1}$.[14,18] This interaction would lead to a significant reduction in ΔK_2 because the near crossings of the energy levels will occur much less pronounced. Further, the exchange interaction may be anisotropic as it was discussed for the direct exchange interactions in other compounds.[32]

A corresponding set of parameters have been used to describe $\Delta K_1/N$ and the hyperfine fields at 4.2 K.[20] The temperature dependence calculated with these data ($\alpha\lambda = -180\ \text{cm}^{-1}$, $g\mu_B H_{\text{exch}} = 370\ \text{cm}^{-1}$, $\Delta_t = 700\ \text{cm}^{-1}$) is shown in Fig. 8 by the dash-dotted line.

C. Magnetostriction

The magnetostriction constants also have been measured by ferromagnetic resonance, by Smith and Jones.[33,34] The experimental conditions thus are the same as in the case of magnetic anisotropy. The field for resonance has been shifted by a compressional stress τ acting on the spheres along the $[1\bar{1}0]$ direction. The applied stress was between 10^7 and $10^8\ \text{dyn cm}^{-2}$, where τ has been calculated using an effective area of the spheres of $\frac{2}{3}\pi R^2$.

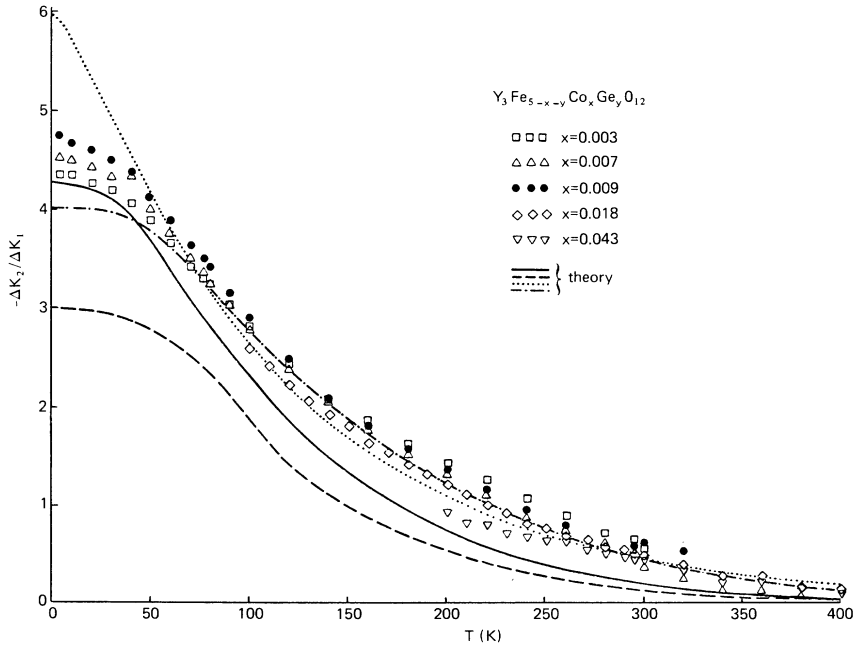

FIG. 8. Measured temperature variation of the ratio of the anisotropy constants for cobalt-substituted yttrium iron garnets. The theoretical curves are discussed in the text.

Then the measured magnetostriction constants of pure yttrium iron garnet are well in accordance with results obtained with other methods.[35] The resonance shifts $\delta H_r([hkl])$ in the principal directions are related to the magnetostriction constants by[34,36]

$$\lambda_{hkl} = -\tfrac{2}{3}(M_s/\tau)\,\delta H_r([hkl]), \quad hkl = 001, 111 \ . \quad (16)$$

At low temperatures we also have the relation

$$\lambda_{111} = -\frac{4}{9}\frac{M_s}{\tau}\left(1+\frac{1}{3}\frac{K_2}{M_s H_r([110])}\right)^{-1} \times\left[\left(1-\frac{2K_1-K_2}{4M_s H_r([110])}\right)\delta H_r([110]) +\frac{1}{2}\left(1-\frac{2K_1}{M_s H_r([110])}\right)\delta H_r([001])\right],$$

which has been used to account for the large anisotropies.

These relations are based on the two-constant magnetoelastic energy of Eq. (4). The magnetostriction constants obtained from the measured resonance shifts via Eq. (16) are plotted versus temperature in Figs. 9(a) and 9(b). Both λ_{100} and λ_{111} are significantly affected by the Co^{2+} ions where $\Delta\lambda_{100}$ is positive and $\Delta\lambda_{111}$ is negative, which agrees with reported data.[25,37,38] The data of sample No. 4 have been omitted in Fig. 9(b) since they overlap with those of sample No. 3 over the complete temperature range. The low temperature measurements for samples Nos. 5 and 6 were prevented by high anisotropy and linewidth. These data indicate a slight reduction of the magnetostrictive effects as it was observed for Fe^{2+}-doped samples.[17] Whether this effect is due to the small Fe^{2+} content in these crystals or to the Co^{2+} ions cannot be decided from the available data. The concentration dependence of the magnetostriction constants is shown in Fig. 10. The dependence on the Co^{2+} content being approximately equal to the total amount of cobalt ions as discussed in Sec. III A is found to be linear in contrast to previous results.[37,38] The contributions $\Delta\lambda_{hkl}/x$ are summarized in Table III together with the data of Fe^{2+},[17] Ru^{3+},[11,39,40] and Mn^{3+},[41,42] being the most effective transition-metal ions, as far as magnetostriction is concerned. The large contribution of Fe^{2+} ions may slightly affect the given low temperature values since they were obtained from the samples with the low-cobalt content.

These results can be compared with the theoretical temperature dependence. The most simple conditions are present for $\Delta\lambda_{100}(T)$ which is displayed in Fig. 11 in a reduced representation. The theoretical curves are calculated from Eq. (12). The solid line is based on the parameter values used for the anisotropy (solid line in Fig. 8). The

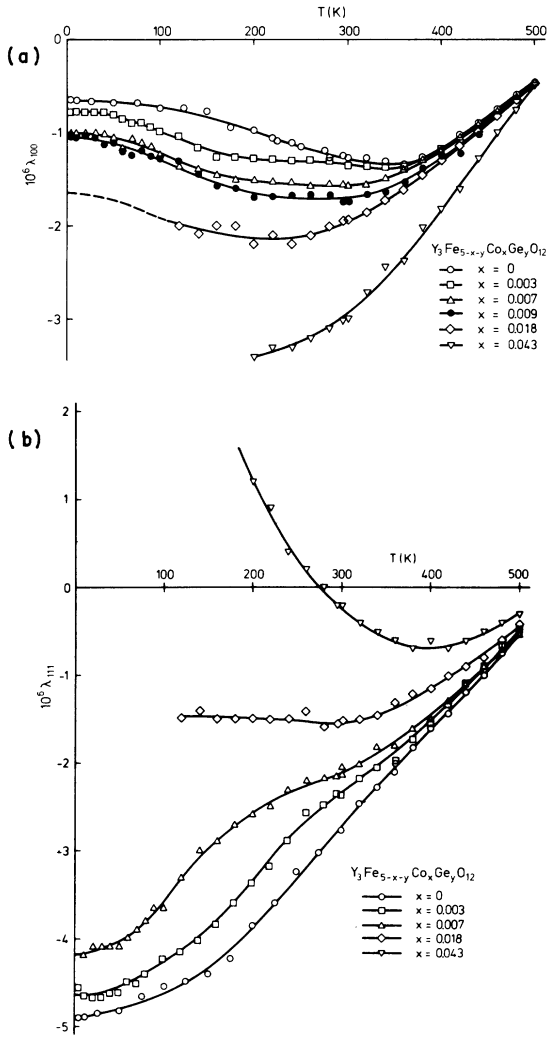

FIG. 9. Temperature variation of the magnetostriction constants (a) λ_{100} and (b) λ_{111} for cobalt-substituted yttrium iron garnets.

dashed line is calculated using a higher exchange field ($g\mu_B H_{exch} = 350\ cm^{-1}$). The experimental data can be described qualitatively. A more quantitative analysis requires additional low temperature measurements of garnets with high cobalt doping to obtain more accurate $\Delta\lambda_{hkl}$ values and an improved theoretical analysis. The comparison with similar results of Ru^{3+} shows that owing to the more simple level structure of this ion, Eqs. (12) and (13) lead to a much better description of the experimental results.[11,40,43]

D. Resonance linewidth

Magnetically anisotropic transition-metal ions like Fe^{2+},[14,18] and Ru^{3+},[29,44] or the rare-earth

ions[45-47] substituted in yttrium iron garnet give rise to strong relaxation. In most cases the experimentally observed linewidth could be well interpreted in terms of the longitudinal relaxation model[48-50] which predicts the following linewidth contribution:

$$\Delta H_l = \frac{N}{4M_s}\sum_{i=1}^{4} P_i \Omega_i \ ,$$

where

$$\Omega_i = \frac{\omega\tau_i}{1+(\omega\tau_i)^2} \ ,$$

$$P_i = \frac{1}{4k_B T}\left[\left(\frac{\partial \Delta E_i}{\partial \theta}\right)^2 + \left(\frac{\partial \Delta E_i}{\partial \varphi}\right)^2\right] \times \frac{1}{\cosh^2(\Delta E_i/2k_B T)} \ . \quad (17)$$

ΔE_i is the energy separation of the two lowest energy levels, ω is the measuring frequency, τ_i is the relaxation time, and the sum extends over the magnetically inequivalent sites. This expression applies for small substitutions and is then proportional to the total number N of relaxing ions. Depending on the relative magnitude of $\omega\tau_i$, different cases with respect to the temperature dependence can be distinguished. At most two temperature maxima of ΔH_l may occur, induced by the functions P_i and Ω_i and in addition a pronounced orientation dependence. In contrast to the results reported in Ref. 2, our measurements strongly support the presence of this relaxation mechanism.

The linear relationship between the measured total cobalt content and the linewidth is well fulfilled, as shown in Fig. 12. This also holds for the spin-wave linewidth as already stated in Sec. III A. The plot of the temperature dependence of the linewidth measured for the three principal directions is displayed in Fig. 13. The typical peaks occurring at different temperatures can be well interpreted

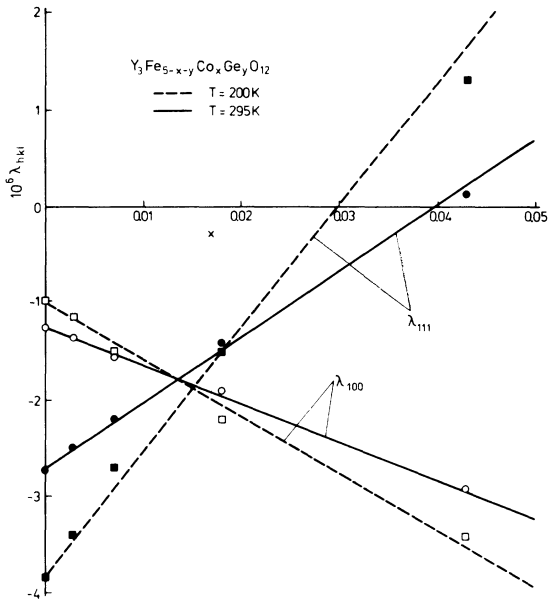

FIG. 10. Concentration dependence of the magnetostriction constants for cobalt-substituted yttrium iron garnets at $T = 200$ K and $T = 295$ K.

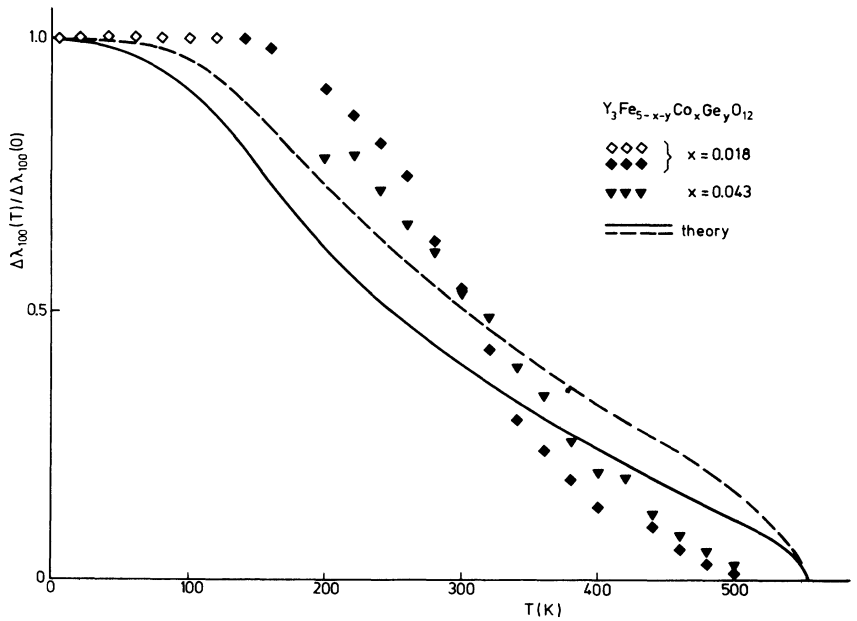

FIG. 11. Relative temperature dependence of the first magnetostriction constant of cobalt-substituted yttrium iron garnets. The open symbols are estimated values from resonance data where the anisotropy and linewidth are quite large. The theoretical curves are calculated from Eq. (12) and are based on $\Delta E(\gamma_1)_{T=0\,K} = 218\ cm^{-1}$ (solid line) and $\Delta E(\gamma_1)_{T=0\,K} = 294\ cm^{-1}$ (dashed line).

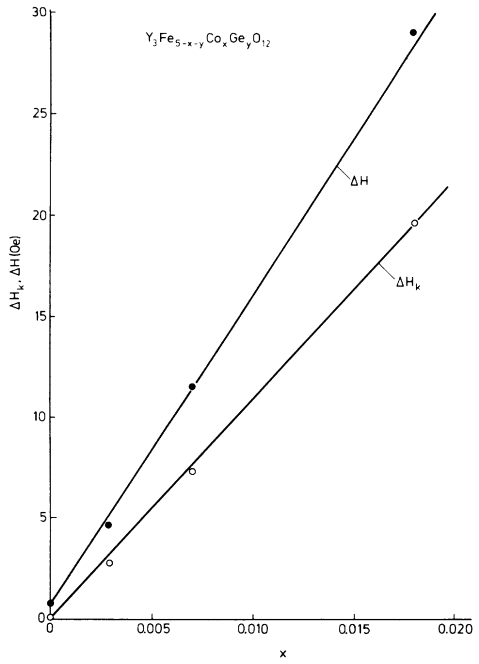

FIG. 12. Linewidth ΔH and spin-wave linewidth ΔH_k in [111] direction vs cobalt concentration in yttrium-iron-garnet single crystals at 9.15 GHz and $T = 295$ K.

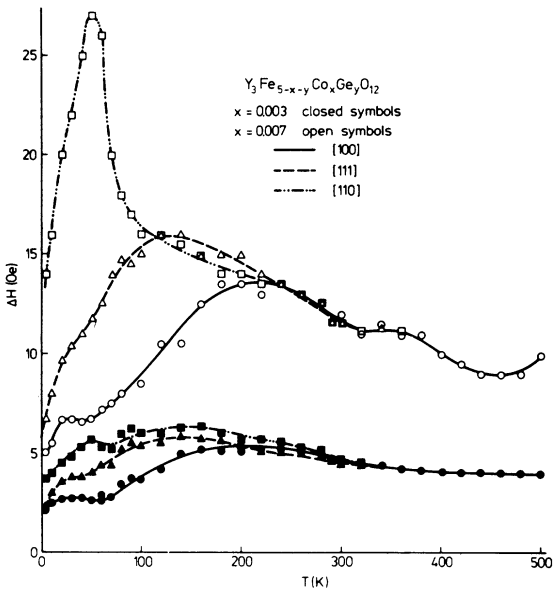

FIG. 13. Temperature variation of the resonance linewidth for cobalt-substituted yttrium iron garnets for the three principal directions.

by Eq. (17) and the orientation dependence of the energy levels shown in Fig. 1.

Except for the magnitude of the energy separations, this orientation dependence is very characteristic and a change of the relative magnitude of the parameters induces only a very small variation in the level structure. The solid line represents the case when the quantization axis is parallel to the [111] direction (γ_1 site). For the two lowest levels also the variation with quantization axis along the $[1\bar{1}\bar{1}]$ direction (γ_2 site) and along the $[\bar{1}11]$ or $[1\bar{1}1]$ direction (γ_3 and γ_4 sites) is shown. The two latter sites are equivalent with respect to the magnetization in the $(1\bar{1}0)$ plane. This orientation dependence is simply correlated to the direction of magnetization by

$$\Delta E_i = \Delta E(\gamma_i)\ , \quad \cos\gamma_1 = \alpha_1 + \alpha_2 + \alpha_3\ , \qquad (18)$$
$$\cos\gamma_2 = -(\alpha_1 + \alpha_2) + \alpha_3\ , \quad \cos\gamma_3 = \alpha_1 - \alpha_2 + \alpha_3\ ,$$

which leads to similar characteristics for all ions where the anisotropy of the lowest levels is essentially governed by a functional dependence on $\cos\gamma_i$. With the aid of Eqs. (17) and (18) and the orientation dependence of the lowest energy levels the experimental data can be discussed. Thereby, our considerations are restricted to a qualitative interpretation since one of the assumptions employed in the derivation of Eq. (17) is the presence of a magnetic doublet being well separated from the higher levels and this does not apply for Co^{2+} ions as obvious from Fig. 1. The maximum linewidth occurs for those orientations where the level separation is minimal. Such minima occurred at the near crossings in the [112] and the [110] direction, when the magnetization is in the $(1\bar{1}0)$ plane. However, in the former case this situation applies only for $\frac{1}{4}$ of the total ions on the γ_1 sites or the γ_2 sites, whereas in the latter case $\frac{1}{2}$ (γ_3 and γ_4 sites) of the Co^{2+} ions give rise to strong relaxation; therefore the linewidth in the [110] direction is expected to be largest. In the [111] direction the energy separation is the same for $\frac{3}{4}$ of the ions (γ_2, γ_3, and γ_4 sites) but slightly larger and therefore the linewidth should be lower. Finally, for the [100] direction all ions exhibit the same energy separation which is larger than in the previous cases and thus the lowest linewidth is expected for this direction. This picture is in accordance with the observed behavior displayed in Fig. 13. The strong dependence of the temperature maximum on the orientation suggests that this is induced by the P_i term. The smaller maximum at higher temperature for sample No. 3 may originate from the Ω_i term. This would correspond to the so-called high-ω case; this maximum may also be induced by the small content of Fe^{2+} ions causing a maximum at 370 K.[14,18] However, this could not be proved since the frequency dependence has not been studied. The P_i term peaks at $kT_m = 0.65\Delta E_i^{\min}$ and

thus the minimum energy separation $\Delta E_i^{\min}$ and the peak temperature T_m roughly can be correlated. From the peak in the [110] direction at $T_m = 55$ K, we estimate T_m values from the energy-level separation for the [111] and [110] directions of 110 K and 192 K, respectively, which agrees pretty well with those observed.

A quantitative analysis becomes much more complex since then we have to take the higher levels into account, requiring a complicated numerical analysis which appears to be useful only in the case where detailed frequency-dependent measurements are available.

IV. CONCLUSIONS

The anisotropic properties of single-crystal garnets of composition $Y_3Fe_{5-x-y}Co_xGe_yO_{12}$ containing essentially divalent cobalt ions have been investigated by ferromagnetic resonance techniques in the temperature range $4.2 \leq T \leq 500$ K. The high concentration of divalent Co^{2+} ions is due to an excess of Ge^{4+} ions which, however, in contrast to other statements in literature is not compensated by Fe^{2+} ions but by other nonmagnetic impurities, such as the Pb^{2+} ion. The limited formation of Fe^{2+} ions is also supported by magnetic circular dichroism measurements on silicon-substituted yttrium iron garnets.[51] Therefore, the low-Fe^{2+} content can be neglected in the interpretation of anisotropy and linewidth phenomena while the low-temperature magnetostriction data may be slightly influenced by these ions because they give rise to large per ion magnetostriction contributions. All magnetic properties strictly vary linearly with Co^{2+} concentration for all temperatures supporting the single-ion behavior as is expected for small concentrations of anisotropic ions. Calculations of the anisotropy and magnetostriction constants in terms of the single-ion model are in qualitative agreement with the experimental results. Improvements of the theory presumably may be obtained if one accounts for the Coulomb interaction arising from the Co^{2+}-Ge^{4+} pairs and possibly the presence of anisotropic exchange.

The temperature dependence of the linewidth exhibits characteristic maxima at low temperatures with a peak temperature depending on the crystallographic direction. The relative peak position can be well understood in terms of the calculated energy level diagram and the longitudinal relaxation mechanism.

ACKNOWLEDGMENTS

The authors are grateful to many colleagues at Philips GmbH Forschungslaboratorium Hamburg for practical help and useful discussions. In particular they wish to thank J. Schuldt for performing the resonance measurements, and Mrs. I. Bartels and F. Welz for the preparation of the crystals.

[1]M. D. Sturge, F. R. Merritt, J.-C. Hensel, and J. P. Remeika, Phys. Rev. 180, 402 (1969).
[2]M. D. Sturge, E. M. Gyorgy, R. C. LeCraw, and J. P. Remeika, Phys. Rev. 180, 413 (1969).
[3]W. P. Wolf, Phys. Rev. 108, 1152 (1957).
[4]K. Yosida and M. Tachiki, Prog. Theor. Phys. 17, 331 (1957).
[5]P. Hansen, J. Schuldt, and W. Tolksdorf, Phys. Rev. B 8, 4274 (1973).
[6]A. Abragam and M. H. L. Pryce, Proc. R. Soc. Lond. A 205, 135 (1951); 206, 173 (1951).
[7]J. C. Slonczewski, Phys. Rev. 110, 1341 (1958).
[8]M. Tachiki, Prog. Theor. Phys. 23, 1055 (1960).
[9]J. C. Slonczewski, J. Phys. Chem. Solids 15, 335 (1960).
[10]J. C. Slonczewski, Phys. Rev. 122, 1367 (1961).
[11]P. Hansen, Phys. Rev. B 8, 246 (1973).
[12]W. Tolksdorf, J. Cryst. Growth 3, 463 (1968).
[13]W. Tolksdorf and F. Welz, J. Cryst. Growth 13, 566 (1972).
[14]P. Hansen, W. Tolksdorf, and J. Schuldt, J. Appl. Phys. 43, 4740 (1972).
[15]J. F. Dillon, Jr., E. M. Gyorgy, and J. P. Remeika, Appl. Phys. Lett. 9, 147 (1966).
[16]D. R. Mack and J. Smit, Appl. Phys. 2, 23 (1973).
[17]P. Hansen, J. Appl. Phys. 48, 801 (1977).
[18]T. S. Hartwick and J. Smit, J. Appl. Phys. 40, 3995 (1969).
[19]The measurements have been carried out by Le Dang Khoi and P. Veillet and are gratefully acknowledged.
[20]LeDang Khoi, P. Veillet, and R. Krishnan, Proceedings of the Eighteenth Ampere Congress, 1974 (unpublished), p. 135.
[21]R. Krishnan, Phys. Status Solidi B 73, K51 (1976).
[22]C. Kittel, Phys. Rev. 76, 743 (1949).
[23]J. O. Artman, Phys. Rev. 105, 62 (1957).
[24]T. Okada, H. Sekizawa, and S. Iida, J. Phys. Soc. Jpn. 18, 981 (1963).
[25]G. F. Dionne and J. B. Goodenough, Mater. Res. Bull. 7, 749 (1972).
[26]P. Hansen, R. Krishnan, and J. Schuldt (unpublished).
[27]P. Hansen and W. Tolksdorf, J. Phys. (Paris) 32, C1-200 (1971).
[28]P. Hansen, Phys. Rev. B 3, 862 (1971).
[29]P. Hansen, Phys. Rev. B 5, 3737 (1972).
[30]J. C. Slonczewski, J. Appl. Phys. 29, 448 (1958).
[31]J. C. Slonczewski, J. Appl. Phys. 32, 253S (1961).
[32]G. M. Copeland and P. M. Levy, Phys. Rev. B 1, 3043 (1970).
[33]A. B. Smith and R. V. Jones, J. Appl. Phys. 34, 1283

(1963).
[34]A. B. Smith, Rev. Sci. Instrum. 39, 378 (1968).
[35]E. DeLacheisserie and J. L. Dormann, Phys. Status Solidi 35, 925 (1969).
[36]G. F. Dionne, J. Appl. Phys. 41, 2264 (1970).
[37]G. A. Petrakovskii, L. M. Protopopova, and E. M. Smokotin, Proc. Intern. Conf. Magnetism (Moscow) 3, 381 (1974).
[38]L. M. Protopopova, G. A. Petrakovskii, É. M. Smokotin, and R. A. Petrov, Sov. Phys.-Solid State 15, 2192 (1974).
[39]R. Krishnan, V. Cagan, and M. Rivoire, AIP Conf. Proc. 5, 704 (1972).
[40]P. Hansen and R. Krishnan, J. Phys. (Paris) 38, C1-147 (1977).
[41]E. M. Gyorgy, J. T. Krause, R. C. LeCraw, L. R. Testarde, and L. G. Van Uitert, J. Appl. Phys. 38, 1226 (1967).
[42]G. F. Dionne and J. B. Goodenough, Mater. Res. Bull. 7, 749 (1972).
[43]E. DeLacheisserie, J. Phys. (Paris) 37, 379 (1976).
[44]P. Hansen, Phys. Status Solidi B 47, 565 (1971).
[45]P. E. Seiden, Phys. Rev. 133, A728 (1964).
[46]B. H. Clarke, K. Tweedale, and R. W. Teale, Phys. Rev. 139, A1930 (1965).
[47]B. H. Clarke, Phys. Rev. 139, A1944 (1965).
[48]A. M. Clogston, Bell. Syst. Tech. J. 34, 739 (1955).
[49]R. W. Teale and K. Tweedale, Phys. Rev. Lett. 1, 298 (1962).
[50]M. Sparks, J. Appl. Phys. 38, 1031 (1967).
[51]P. Paroli and S. Geller, J. Appl. Phys. 48, 1364 (1977).